

## **BULK MODELS OF THE ATMOSPHERIC CONVECTIVE BOUNDARY LAYER**

E. FEDOROVICH

*Institute of Hydrology and Water Resources Planning  
Karlsruhe University  
Kaiserstrasse 12, 76128 Karlsruhe, Germany*

### **Abstract**

The paper presents an overview of modeling the atmospheric convective boundary layer (CBL) using bulk parameterizations for the vertical structure of the layer. Such parameterizations are constructed based on empirical knowledge about vertical distributions of meteorological variables in the CBL.

Two main types of CBL bulk models are presented and discussed. The first model considered is the so-called zero-order jump model, which implies a vertical homogeneity of meteorological variables in the bulk of the CBL, and zero-order discontinuities of variables at the interfaces of the layer. Integral budgets of momentum and heat in the zero-order jump model of the dry atmospheric CBL are considered. A general version of the equation describing the CBL growth rate (the entrainment rate equation) is obtained through integration of the turbulence kinetic energy balance equation, evoking basic assumptions of the zero-order representation of the CBL vertical structure. The developed theory is generalized for the case of the CBL over an irregular terrain.

The second model considered is the general-structure CBL bulk model, which incorporates a self-similar representation of the buoyancy profile within the capping inversion layer. This representation has been examined against the data from atmospheric measurements, laboratory experiments with buoyancy agitated turbulence, and large eddy simulations. The growth rate equations for mixed and inversion layers are derived using the turbulence kinetic energy balance equation and the Deardorff scaling hypothesis refined to account for the inversion-layer structure. The model is found to be able to reproduce transition regimes of the CBL development affected by nonstationarity of the entrainment zone.

### **1. Introduction**

Studies of the atmospheric convective boundary layer (CBL) within the framework of bulk-model methodology have passed through several historical stages. Most

extensively, the CBL was studied with the so-called zero-order jump models originating from the pioneering works of Ball [1] and Lilly [28].

According to the zero-order jump model, the potential temperature within the CBL is presumed to be height constant. Its changes with height in the surface layer, and in the entrainment layer at the CBL top are reduced to the zero-order discontinuities of the temperature profile. The analogous zero-order parameterization is employed for the wind velocity profile (Garraat *et al.* [22]). Wind velocity in the CBL is taken to be uniform with height. Velocity shears across the surface layer and in the entrainment layer are represented by steps in the wind profile. The vertical structure of the velocity and temperature fields in the stably stratified free-atmosphere layer above the CBL is assumed to be known.

The breakthrough in the zero-order jump modeling of the CBL happened in the seventies when Plate [38], Betts [4], Carson [7], Tennekes [47], Stull [42-44], Carson and Smith [8], Zilitinkevich [52], and Zeman and Tennekes [51] proposed a set of zero-order jump approaches for modeling a horizontally homogeneous, shear-free CBLs. Later, Zilitinkevich [54] suggested a generalized zero-order jump CBL model, comprising the aforementioned models as asymptotic cases. Several applied mesometeorological models, *e.g.* those of Kraus and Leslie [26], Brutsaert [6], Batchvarova and Gryning [2], and Zilitinkevich *et al.* [55] were developed based on the zero-order parameterization of the CBL vertical structure. Most of those models dealt with a horizontally homogeneous CBL and used simplifying assumptions concerning the effects of wind shear.

In an attempt to reproduce the CBL vertical structure in a more detailed way, higher-order bulk models of the CBL were proposed. In the first-order jump model, Betts [5] introduced the interfacial layer of finite thickness between the mixed layer and the free atmosphere. The potential temperature profile was taken to be linear in this layer, undergoing first-order discontinuities at its upper and lower boundaries. The general-structure CBL bulk models of Deardorff [13], and Fedorovich and Mironov [21] provided for realistic representation of the temperature / buoyancy profile in the entrainment zone, accounting for nonstationarity of the entrainment. All mentioned models of higher orders were proposed for shear-free cases of the atmospheric CBL.

Within the last two decades, modeling activities in the CBL area have switched almost entirely to large eddy numerical simulations. Although the first large eddy simulation (LES) of the atmospheric CBL has been already performed by J. Deardorff during the early seventies (Deardorff [9, 11-12]), progress in the field was slow due to the lack of computer power and insufficient capacity of data storage devices. In the eighties, the situation had improved, and significant results in LES studies of the atmospheric CBL were achieved. Most notable are the works of Moeng [31-33], Nieuwstadt and Brost [37], Moeng and Wyngaard [35], Mason [30], Schmidt and Schumann [41], and Moeng and Sullivan [34]. Different types of the CBL and various features of its structure have been investigated with the aid of LES during the last fifteen years.

However, although being very valuable and efficient tools for fundamental studies of the atmospheric convection, and possessing the same ability in reproducing fine features of the flow structure as high-resolution laboratory experiments, the LES

models can hardly be used at present for applied purposes due to the enormous computer resources they still demand.

This is one of the reasons why the bulk approach remains to be an attractive model framework for applied studies of the atmospheric CBL.

## 2. Zero Order Jump Model

A zero-order jump parameterization for the vertical structure of the atmospheric CBL is presented in Fig. 1. It is based on the observed features of vertical distributions of meteorological variables in the CBL which are extensively discussed in a number of contributions to this ASI volume, see *e.g.* papers by Lenschow [27], Plate [39], and Fedorovich and Kaiser [20]. The main feature is the strong turbulent mixing embracing the whole layer and causing the approximate uniformity of the vertical distribution of physical substances within the CBL. Thus, within the zero-order approach, the CBL is represented by the convectively mixed layer with two interfaces, the upper one (at  $z=h$ ) and the lower one (at  $z=0$ ), across which the potential temperature and wind velocity change in a jumplike way.

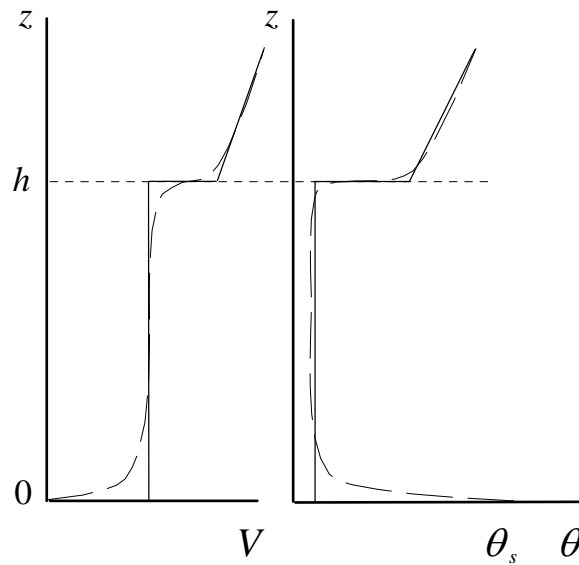


Figure 1. Actual (dashed lines) and zero-order jump (solid lines) profiles of wind velocity  $V$ , and potential temperature  $\theta$  in the convective boundary layer;  $\theta_s$  is the near-surface value of  $\theta$ .

In historical retrospective, the ideology of zero-order jump modeling was mainly developed for the case of horizontally homogeneous, shear-free atmospheric CBL. For the CBL with wind shear, quite a few parameterizations have been suggested. Some of them are reviewed in Stull [46]. The effects of baroclinicity (thermal wind), advection, and horizontal diffusion, which can be important for forming the meteorological regime of the atmospheric CBL, were left beyond the scope of traditional zero-order

jump model studies. A theoretical framework for applied zero-order jump CBL modeling, which takes into account the above effects, has been proposed by Fedorovich [19]. In the following subsections, particular features of this model framework will be considered.

### 2.1. HEAT AND MOMENTUM BUDGETS IN ZERO ORDER CBL MODEL

The following initial equations written in the Reynolds form describe the flow in the nonstationary, horizontally inhomogeneous atmospheric CBL.

The momentum balance equations:

$$\frac{\partial u}{\partial t} + \frac{\partial uu}{\partial x} + \frac{\partial vu}{\partial y} + \frac{\partial wu}{\partial z} = f(v - v_{g0} - \Gamma_v z) + \frac{\partial \tau_x}{\partial z}, \quad (1)$$

$$\frac{\partial v}{\partial t} + \frac{\partial uv}{\partial x} + \frac{\partial vv}{\partial y} + \frac{\partial wv}{\partial z} = -f(u - u_{g0} - \Gamma_u z) + \frac{\partial \tau_y}{\partial z}, \quad (2)$$

where  $u$ ,  $v$  and  $w$  are the components of mean wind velocity along axes  $x$ ,  $y$  and  $z$ , respectively;  $\tau_x = -\langle w' u' \rangle$  and  $\tau_y = -\langle w' v' \rangle$  are components of the vertical turbulent flux of momentum normalized by density, the sign  $\langle \dots \rangle$  denotes the operation of Reynolds averaging;  $f$  is the Coriolis parameter;  $u_{g0}$  and  $v_{g0}$  are the near-surface values of the geostrophic wind components,  $\Gamma_u$  and  $\Gamma_v$  are the vertical gradients of these components. The last four quantities at this point are presumed to be prescribed functions of time and horizontal coordinates. Later we shall show a way of determining them from pressure and temperature spatial distributions. Equations (1) and (2) imply that contribution of the horizontal turbulent transport to the momentum balance is negligible compared to vertical turbulent transport, and conditions of hydrostatic equilibrium are satisfied in the CBL (Qi *et al.* [40]). These assumptions hold when horizontal scales in the flow dominate over the vertical ones which is typical for most of the CBL cases observed in nature and simulated in the laboratory.

The mass conservation equation is employed in the form:

$$\frac{\partial u}{\partial x} + \frac{\partial v}{\partial y} + \frac{\partial w}{\partial z} = 0. \quad (3)$$

In the heat transfer equation

$$\frac{\partial \theta}{\partial t} + \frac{\partial u\theta}{\partial x} + \frac{\partial v\theta}{\partial y} + \frac{\partial w\theta}{\partial z} = -\frac{\partial Q}{\partial z}, \quad (4)$$

where  $\theta$  is the mean potential temperature, and  $Q = \langle w' \theta' \rangle$  is the turbulent kinematic heat flux, the following assumption, which is analogous to the one used in the momentum balance equations, is made: the advection and the vertical turbulent

transport ultimately dominate the horizontal turbulent exchange. In Eq. (4), we also neglected the contributions of molecular and radiation heat transfer to the heat balance of the CBL. The first one is very small in the atmosphere compared to the turbulent heat transfer, whereas the radiation effects are omitted for simplicity. Principally, they can be incorporated in the CBL zero-order jump model, see *e.g.* Zilitinkevich *et al.* [55].

The above equations correspond to the general case of the CBL over a flat underlying surface. To obtain the equations of the momentum and heat budget of the layer, we integrate Eqs. (1), (2), and (4) over the boundary-layer depth, *i.e.* over  $z$  from 0 to  $h$ , taking into account the zero-order jump representations of the temperature and velocity profiles, see Fig. 1. As we integrate, we will include the zero-order discontinuity surface in the integration domain, thus regarding the upper side of this surface as the CBL edge.

Calculating the integrals from each term of the first equation of motion, we come to the equation of the integral budget of momentum along the  $x$  axis, (see derivation in Fedorovich [19]):

$$h \left( \frac{\partial \bar{u}}{\partial t} + \bar{u} \frac{\partial \bar{u}}{\partial x} + \bar{v} \frac{\partial \bar{u}}{\partial y} \right) = \Delta u \frac{Dh}{Dt} + h \left[ f(\bar{v} - v_{g0}) - \frac{h}{2} f \Gamma_v \right] - \tau_{xs}. \quad (5)$$

where  $\bar{u}$  is the average value of the  $x$  component of wind velocity within the mixed layer;  $\Delta u = u_h - \bar{u}$  is the increment of this component across the mixed-layer upper interface;  $u_h$  is the value of  $u$  in the stable layer, at the upper side of the zero-order interface represented by the surface of zero-order discontinuity;  $\frac{Dh}{Dt} \equiv \frac{\partial h}{\partial t} + \bar{u} \frac{\partial h}{\partial x} + \bar{v} \frac{\partial h}{\partial y}$  is the substantial (total) variation of  $h$ . The operation of

averaging over the mixed-layer depth is defined here as  $\bar{(\quad)} = \frac{1}{h} \int_0^h (\quad) dz$ .

The variation  $Dh/Dt$  in fact describes the combined effect of three mechanisms determining the evolution of the CBL depth. The first of them, represented by  $\partial h / \partial t$ , is associated with local changes of  $h$  (nonstationarity). Horizontal advection constitutes the second mechanism. It contributes to the total variation by  $\bar{u}(\partial h / \partial x) + \bar{v}(\partial h / \partial y)$ . The third mechanism is the subsidence related to the horizontal divergence of the flow in the CBL:  $h[(\partial \bar{u} / \partial x) + (\partial \bar{v} / \partial y)] = -w_{hs}$ , where  $w_{hs}$  is the subsidence velocity at the CBL top. The subsidence velocity is a part of

$$w_h = - \int_0^h \frac{\partial u}{\partial x} dz - \int_0^h \frac{\partial v}{\partial y} dz = - \frac{\partial \bar{u} h}{\partial x} + u_h \frac{\partial h}{\partial x} - \frac{\partial \bar{v} h}{\partial y} + v_h \frac{\partial h}{\partial y},$$

which is the total vertical velocity at  $z=h$ .

Integration of the second equation of motion (2), and of the heat balance equation (4) gives (Fedorovich [19])

$$h \left( \frac{\partial \bar{v}}{\partial t} + \bar{u} \frac{\partial \bar{v}}{\partial x} + \bar{v} \frac{\partial \bar{v}}{\partial y} \right) = \Delta v \frac{Dh}{Dt} - h \left[ f(\bar{u} - u_{g0}) - \frac{h}{2} f\Gamma_u \right] - \tau_{ys} \quad (6)$$

and

$$h \left( \frac{\partial \bar{\theta}}{\partial t} + \bar{u} \frac{\partial \bar{\theta}}{\partial x} + \bar{v} \frac{\partial \bar{\theta}}{\partial y} \right) = \Delta \theta \frac{Dh}{Dt} + Q_s, \quad (7)$$

respectively. The latter expression, in which  $Q_s$  is the near-surface value of the kinematic heat flux, presents the heat budget of the CBL.

For now we shall consider  $Q_s$ , as well as the components  $\tau_{xs}$  and  $\tau_{ys}$  of the near-surface shear stress to be known functions of time and the horizontal coordinates. In section 2.5, some approaches towards specifying these characteristics in the zero-order jump models of the CBL will be presented.

## 2.2. PROFILES OF TURBULENT FLUXES

The expressions of the momentum and heat-flux profiles are derived by integrating Eqs. (1), (2), and (4) over the vertical co-ordinate from 0 to  $z$ . From the Eq. (1), we have for the  $x$  component of the momentum flux:

$$\tau_x = \tau_{xs} + \int_0^z \left( \frac{\partial u}{\partial t} + \frac{\partial uu}{\partial x} + \frac{\partial uv}{\partial y} + \frac{\partial wu}{\partial z} \right) dz - \int_0^z f(v - v_{g0} - \Gamma_v z) dz.$$

Employing the zero-order jump representation of the velocity profile and evaluating  $w$  by integration of the continuity equation (3) from 0 to  $z$ , we obtain  $\tau_x$  as the quadratic function of  $z$ :

$$\tau_x = \tau_{xs} + z \left( \frac{\partial \bar{u}}{\partial t} + \bar{u} \frac{\partial \bar{u}}{\partial x} + \bar{v} \frac{\partial \bar{u}}{\partial y} \right) - z \left[ f(\bar{v} - v_{g0}) - \frac{z}{2} f\Gamma_v \right],$$

which can be written in the form (Fedorovich [19]):

$$\tau_x = \tau_{xs} (1 - \zeta) + \Delta u \frac{Dh}{Dt} \zeta + \frac{h^2}{2} f\Gamma_v \zeta (\zeta - 1), \quad (8)$$

where  $\zeta = z/h$  is the dimensionless height.

Similarly, the expressions of the  $y$  component of the momentum flux

$$\tau_y = \tau_{ys}(1 - \zeta) + \Delta v \frac{Dh}{Dt} \zeta - \frac{h^2}{2} f \Gamma_u \zeta (\zeta - 1), \quad (9)$$

and of the heat flux

$$Q = Q_s(1 - \zeta) - \Delta \theta \frac{Dh}{Dt} \zeta \quad (10)$$

profiles as functions of dimensionless height can be obtained. It is seen from Eq. (10) that kinematic heat flux in the zero-order jump CBL model changes linearly with height.

Equations (8), (9), and (10) indicate that both components of the momentum flux, as well as the heat flux, undergo the zero-order discontinuities at the mixed-layer interface. Just below this surface they reach the values  $\Delta u \frac{Dh}{Dt}$ ,  $\Delta v \frac{Dh}{Dt}$ , and  $-\Delta \theta \frac{Dh}{Dt}$ , respectively. From the upper side of the discontinuity surface all turbulent fluxes vanish.

### 2.3. ENTRAINMENT RATE EQUATION

The CBL depth  $h$  is one of the most important variables characterizing the process of convection. Due to the penetration of thermals into the stably stratified flow above the mixed layer, the heat and momentum from the stable region are entrained or mixed down into the bulk of the turbulent convective layer. The entrainment is thus the principal mechanism responsible for the CBL growth dynamics.

To describe variations of  $h$  in time and space we depart from the turbulent kinetic energy (TKE) balance equation. In the case under consideration, this equation has the form

$$\frac{\partial e}{\partial t} + \frac{\partial ue}{\partial x} + \frac{\partial ve}{\partial y} + \frac{\partial we}{\partial z} = \tau_x \frac{\partial u}{\partial z} + \tau_y \frac{\partial v}{\partial z} + \beta Q - \frac{\partial \Phi}{\partial z} - \varepsilon, \quad (11)$$

where  $e$  is the TKE per unit mass,  $\varepsilon$  is the energy dissipation rate, and  $\Phi$  is the vertical transport of energy due to turbulent exchange and pressure fluctuations.

To obtain the entrainment rate equation, we integrate Eq. (11) over  $z$  from 0 to  $h$ . The integration of the left-hand part, representing the temporal variations of  $e$  and its transformations due to advection, yields

$$\int_0^h \left( \frac{\partial e}{\partial t} + \frac{\partial ue}{\partial x} + \frac{\partial ve}{\partial y} + \frac{\partial we}{\partial z} \right) dz = \frac{\partial}{\partial t} \bar{e}h + \frac{\partial}{\partial x} \bar{e}uh + \frac{\partial}{\partial y} \bar{e}vh.$$

While deriving the above expression, we set  $e_h = 0$ , since the zero-order jump model assumes that turbulence vanishes at  $z=h$ .

The integration of the shear production terms in the right-hand part of (11) cannot be carried out directly because we have to integrate the products of the shear stress components (which are discontinuous at  $z=h$ ) and vertical derivatives of the velocity components (they are infinite at  $z=0$  and  $z=h$  within the framework of the zero-order parameterization). The following approach for calculating the integrals can be applied (we shall demonstrate it using the first term as an example).

In the vicinity of  $h$  we isolate a thin layer with the depth  $\delta h$ . Then we approximate the velocity gradient across this layer with  $\Delta u / \delta h$ , and the increment of the  $x$  component of momentum flux with the linear function  $\Delta u \frac{Dh}{Dt} \frac{h-z}{\delta h}$ , multiply them, and carry out the integration over the layer  $\delta h$ . This yields  $\frac{1}{2} \Delta u^2 \frac{Dh}{Dt}$ , the value of the integral being independent on  $\delta h$ . Therefore it holds true when  $\delta h$  tends to zero. While calculating the integral over the rest of the mixed layer we should take into account that in the bulk of the layer velocity is height constant, and therefore there is no shear production of turbulent kinetic energy in this region. The contribution of shear in the thin near-surface layer, where velocity sharply increases from zero to the value characteristic of the mixed layer, and where variation of the momentum flux with height is negligibly small, can be evaluated analogous to the way used in the vicinity of  $h$ . It is easy to show that such integration results in  $\bar{u} \tau_{xs}$ .

Thus, for the integral TKE production by shear we obtain:

$$\int_0^h \left( \tau_x \frac{\partial u}{\partial z} + \tau_y \frac{\partial v}{\partial z} \right) dz = \bar{u} \tau_{xs} + \bar{v} \tau_{ys} + \frac{1}{2} (\Delta u^2 + \Delta v^2) \frac{Dh}{Dt}.$$

The integral TKE production by buoyancy forces is expressed as

$$\int_0^h \beta Q dz = \beta \frac{h}{2} \left( Q_s - \Delta \theta \frac{Dh}{Dt} \right).$$

We assume that there is no transport of energy through the underlying surface. Therefore the integral of the transport term yields  $-\Phi_h$ , which is the negative flux of energy at the CBL top. Within the employed model framework, the energy drain at  $z=h$  should be associated solely with the internal gravity waves (Zilitinkevich [54]), (see also section 3.2), since the zero-order jump model postulates vanishing of turbulent transport above  $h$ . It was noted by Stull [45] that for typical atmospheric CBL cases the energy drain by gravity waves is relatively small. On the other hand, Fedorovich and Mironov [21] have found a pronounced effect of the energy transport by waves in the CBL case with rather moderate stable stratification in the turbulence-free flow region aloft.

Summarizing the above expressions for the different components of the integral TKE balance, we come to the entrainment equation

$$\left[ \bar{e} - \frac{1}{2}(\Delta u^2 + \Delta v^2 - \beta h \Delta \theta) \right] \frac{Dh}{Dt} + \left( \frac{\partial \bar{e}}{\partial t} + \bar{u} \frac{\partial \bar{e}}{\partial x} + \bar{v} \frac{\partial \bar{e}}{\partial y} - \frac{\beta}{2} Q_s + \bar{\varepsilon} \right) h = \bar{u} \tau_{xs} + \bar{v} \tau_{ys} - \Phi_h. \quad (12)$$

To solve this equation, one should specify a way of evaluating the mixed-layer means  $\bar{e}$  and  $\bar{\varepsilon}$ , and also a method of calculating the transport of energy  $\Phi_h$  at the mixed-layer top. Within the zero-order approach these variables are commonly determined using parameterizations based on similarity arguments.

In the most studied case of the nonsteady, horizontally quasi-homogeneous, shear-free CBL, the entrainment equation (12) reduces to

$$\left( \bar{e} + \frac{\beta h \Delta \theta}{2} \right) \frac{dh}{dt} + \left( \frac{d\bar{e}}{dt} + \bar{\varepsilon} - \frac{\beta}{2} Q_s \right) h = -\Phi_h. \quad (12a)$$

For the shear-free CBL, traditional parameterizations for  $\bar{e}$  and  $\bar{\varepsilon}$  result from the Deardorff [10] self-similarity hypothesis, which states that profiles of  $e$  and  $\varepsilon$  normalized using  $h$  as the height scale and  $w_* = (\beta Q_s h)^{1/3}$  as the velocity scale are universal functions of the dimensionless height  $\zeta = z/h$ . This allows the representations  $\bar{e} = C_e (\beta Q_s h)^{2/3}$  for the mean TKE, and  $\bar{\varepsilon} = C_\varepsilon \beta Q_s$  for the mean dissipation rate, where  $C_e$  and  $C_\varepsilon$  are universal constants.

From the analysis of water tank and atmospheric experimental data, Zilitinkevich [54] found these constants to be 0.5 and 0.4, respectively. Fedorovich and Mironov [21], who additionally employed data from several LES studies of the shear-free CBL, has shown that these estimates are apparently exaggerated by 25%. This could be due to the disturbing presence of shear during field measurements and parasite enhancement of horizontal velocity fluctuations by bottom temperature variations in the water tank experiments.

For the vertical transport of energy from the CBL top, the two most known parameterizations were suggested, the first of Kantha [25], and the second of Zilitinkevich [54]. Both are based on the relationship of Thorpe [49], who expressed the energy drain from the CBL through the parameters of the waves propagating in the nonturbulent fluid above the layer. Parameterization of Kantha, accompanied by the geometric formula of Stull [44] relating the so-called entrainment coefficient  $A = \frac{\Delta \theta (dh/dt)}{Q_s}$  to the ratio  $(\Delta h/2)/(h - \Delta h/2)$ , where  $\Delta h$  is the entrainment-zone depth, results in

$$\Phi_h = C_{Nh} N^3 h^3 \left( \frac{A}{1+A} \right)^2,$$

whereas the Zilitinkevich parameterization gives

$$\Phi_h = C_{Nh}' N^3 h^3 \left( \frac{A}{1+A} \right)^3.$$

In the above expressions,  $C_{Nh}$  and  $C_{Nh}'$  are dimensionless constants. Zilitinkevich [54] estimated  $C_{Nh}'$  to be 0.02. From the experiments with a general-structure CBL model, Fedorovich and Mironov [21] found that  $C_{Nh}$  is about one order of magnitude smaller than  $C_{Nh}'$ .

Further simplification of the entrainment equation commonly involves omitting the  $\bar{\epsilon}$  containing terms in the left-hand side of Eq. (12a), and neglecting the wave-related energy flux in its right-hand side. This provides a closure relationship

$$A = \frac{\Delta\theta \frac{dh}{dt}}{Q_s} = 1 - 2C_\epsilon = const, \quad (12b)$$

where the value of constant is set equal 0.2. The last expression works decently for the CBL cases when the simplifications made are justified.

For the CBL with wind shear, a general parameterization of  $\Phi_h$  has not yet been proposed. In this case, the employment of the geometric formula [44] for determination of  $\Delta h$  is becoming questionable because it does not take into account the influence of shear on the entrainment-zone dynamics. One of the feasible solutions is to use the diagnostic relationship between the normalized entrainment zone depth,  $\Delta h / h$ , and a dimensionless parameter of entrainment  $Ri_E = \beta \Delta\theta (dh / dt)^{-2} h$ , suggested by Gryning and Batchvarova [23] and tested later in their applied model for the height of the daytime mixed layer and the entrainment zone (Batchvarova and Gryning [3]):  $\Delta h / h = 3.3 Ri_E^{-1/3} + 0.2$ .

Applied CBL models based on the bulk approach usually employ a stationary version of the TKE balance equation (Stull [43], Zilitinkevich *et al.* [55], and Gryning and Batchvarova [23]). This enables one to avoid the problem of parameterizing  $\bar{\epsilon}$ , but leaves the problem of  $\bar{\epsilon}$  determination open. In most of suggested applied models,  $\bar{\epsilon}$  is merely set equal to combination of the TKE integral production components, each taken with an empirical proportionality coefficient (Stull [43], Tennekes and Driedonks [48], Driedonks [17], Driedonks and Tennekes [18], and Batchvarova and Gryning [2]). The shear forcing at the CBL bottom is parameterized in these models through  $u_*^3$ , and the effect of the elevated shear is expressed in terms of  $(\Delta\bar{V})^3$ , where  $u_* = \sqrt[4]{\tau_{xs}^2 + \tau_{ys}^2}$  is the friction velocity, and  $\Delta\bar{V}$  is the wind shear across the CBL top. As one can infer from Eq. (12), the direct integration of TKE balance equation, evoking the assumptions of zero-order jump approach, yields quite different expressions for the shear production terms:  $\bar{u} \tau_{xs} + \bar{v} \tau_{ys}$  (at the bottom), and

$\frac{1}{2}(\Delta u^2 + \Delta v^2) \frac{Dh}{Dt}$  (at the upper interface). Generally, even for average conditions, it is not as evident whether  $\bar{u} \tau_{xs} + \bar{v} \tau_{ys}$  can be taken proportional to  $u_*^3$ , and  $\frac{1}{2}(\Delta u^2 + \Delta v^2) \frac{Dh}{Dt}$  to  $(\Delta \bar{V})^3$ . It is also easy to notice that the first of the last two terms always remains positive during the convective-layer growth, whereas the second has the sign of  $\Delta \bar{V}$  and thus can be a sink of TKE in the growing CBL.

#### 2.4. ATMOSPHERIC CBL OVER IRREGULAR TERRAIN

Under common atmospheric conditions, the convective boundary layer develops over an underlying surface with variable topography, roughness, and thermal properties. If these variations are not very sharp in space, it is possible to generalize the above theory for the case when lower interface of the CBL is represented by some known function  $H=H(x, y)$  describing the topography, and the spatial distribution of aerodynamic roughness is given by  $z_{0u}(x, y)$ , see Fig. 2.

The initial equations for the case under consideration slightly differ from the model equations corresponding to the case of the CBL over the flat surface. In the momentum balance equations (1) and (2) the first terms in the right-hand parts must be modified in the following way:

$$\begin{aligned} & f \left[ v - v_{g0} - \Gamma_v(z - H) \right], \\ & - f \left[ u - u_{g0} - \Gamma_u(z - H) \right], \end{aligned}$$

since the near-surface values of the geostrophic wind are now prescribed at the level  $H(x, y)$ . Functions  $\Gamma_v$  and  $\Gamma_u$  become the internal parameters of the model. We shall indicate in section 2.5 the method of evaluating them from the temperature field. The mass consistency and the heat balance are expressed, as previously, by relationships (3) and (4), respectively.

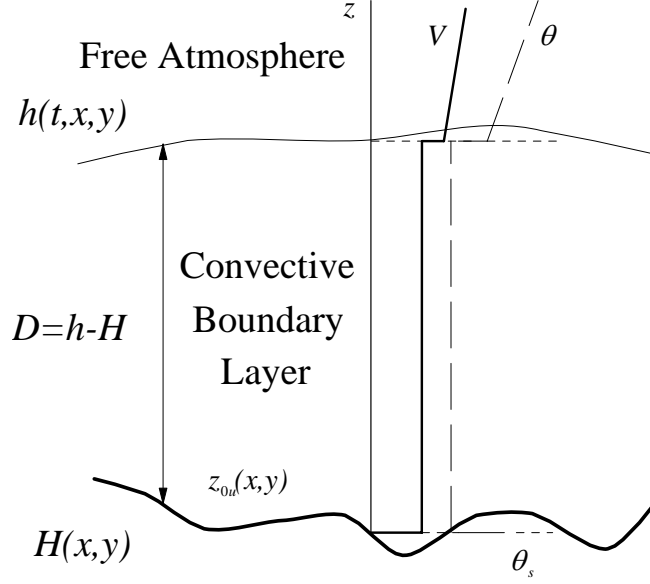


Figure 2. Schematic of the atmospheric convective boundary layer over irregular terrain.

We transform the co-ordinate system by introducing new time and space variables

$$t_n = t, \quad x_n = x, \quad y_n = y, \quad z_n = \frac{z - H(x, y)}{h(t, x, y) - H(x, y)},$$

where new variables are denoted by subscript  $n$ .

In the transformed co-ordinates, the first equation of motion can be integrated over  $z_n$ , see Fedorovich [19], which yields the momentum-budget equation

$$D \left( \frac{\partial \bar{u}}{\partial t} + \bar{u} \frac{\partial \bar{u}}{\partial x} + \bar{v} \frac{\partial \bar{u}}{\partial y} \right) = \Delta u \left( \frac{\partial h}{\partial t} + \frac{\partial \bar{u} D}{\partial x} + \frac{\partial \bar{v} D}{\partial y} \right) + D \left[ f(\bar{v} - v_{g0}) - \frac{D}{2} f \Gamma_v \right] - \tau_{xs}. \quad (13)$$

In the above expression,  $D(t, x, y) = h - H$  is the relative CBL depth, and the averaging is defined through integration over the dimensionless vertical coordinate. Equation (13) is quite similar to Eq. (5) presenting the integral balance of the  $x$  component of momentum in the CBL over the flat surface.

The equation of the momentum balance along the  $y$  axis

$$D \left( \frac{\partial \bar{v}}{\partial t} + \bar{u} \frac{\partial \bar{v}}{\partial x} + \bar{v} \frac{\partial \bar{v}}{\partial y} \right) = \Delta v \left( \frac{\partial h}{\partial t} + \frac{\partial \bar{u} D}{\partial x} + \frac{\partial \bar{v} D}{\partial y} \right) - D \left[ f(\bar{u} - u_{g0}) - \frac{D}{2} f \Gamma_u \right] - \tau_{ys}, \quad (14)$$

and the integral heat balance equation

$$D \left( \frac{\partial \bar{\theta}}{\partial t} + \bar{u} \frac{\partial \bar{\theta}}{\partial x} + \bar{v} \frac{\partial \bar{\theta}}{\partial y} \right) = \Delta \theta \left( \frac{\partial h}{\partial t} + \frac{\partial \bar{u} D}{\partial x} + \frac{\partial \bar{v} D}{\partial y} \right) + Q_s, \quad (15)$$

can be obtained analogously.

Integration of the momentum balance, and heat transfer equations over the normalized vertical coordinate from 0 to  $z_n$  yields expressions of the momentum flux components and turbulent heat flux as functions of  $z_n$ :

$$\tau_x = \tau_{xs}(1 - z_n) + \Delta u \left( \frac{\partial h}{\partial t} + \frac{\partial \bar{u} D}{\partial x} + \frac{\partial \bar{v} D}{\partial y} \right) z_n + \frac{D^2}{2} f \Gamma_v z_n (z_n - 1), \quad (16)$$

$$\tau_y = \tau_{ys}(1 - z_n) + \Delta u \left( \frac{\partial h}{\partial t} + \frac{\partial \bar{u} D}{\partial x} + \frac{\partial \bar{v} D}{\partial y} \right) z_n + \frac{D^2}{2} f \Gamma_v z_n (z_n - 1), \quad (17)$$

$$Q = Q_s(1 - z_n) - \Delta \theta \left( \frac{\partial h}{\partial t} + \frac{\partial \bar{u} D}{\partial x} + \frac{\partial \bar{v} D}{\partial y} \right) z_n. \quad (18)$$

Substituting the above expressions in the TKE balance equation (11) written in the new coordinate system, and carrying out the termwise integration of this equation in a way similar to that shown in section 2.3, we obtain a version of the entrainment rate equation for the atmospheric CBL over irregular terrain:

$$\begin{aligned} & \left[ \bar{\varepsilon} + \frac{1}{2} (\Delta u^2 + \Delta v^2 - \beta h \Delta \theta) \right] \left( \frac{\partial h}{\partial t} + \frac{\partial \bar{u} D}{\partial x} + \frac{\partial \bar{v} D}{\partial y} \right) \\ & + \left( \frac{\partial \bar{\varepsilon}}{\partial t} + \bar{u} \frac{\partial \bar{\varepsilon}}{\partial x} + \bar{v} \frac{\partial \bar{\varepsilon}}{\partial y} - \frac{\beta}{2} Q_s + \bar{\varepsilon} \right) D = \bar{u} \tau_{xs} + \bar{v} \tau_{ys} - \Phi_h, \end{aligned} \quad (19)$$

This equation differs in merely a few details from the entrainment rate equation for the CBL over a flat surface, see Eq. (12).

## 2.5. EXTERNAL PARAMETERS

In atmospheric boundary-layer modeling, the value of the near-surface heat flux  $Q_s$  is usually derived from the equation of the surface heat balance, provided the methods of evaluating the other balance components are known. The simple algorithm for this purpose was proposed in Zilitinkevich *et al.* [55]. This algorithm incorporates the

expression relating  $\bar{\theta}$  to the near-surface value of temperature  $\theta_s$ , and a formula for calculating the roughness parameter with respect to the temperature.

Departing from the value of  $Q_s$ , and from the roughness parameter with respect to the wind,  $z_{0u}(x,y)$ , the components of the near-surface momentum flux  $\tau_{xs}$  and  $\tau_{ys}$  can be evaluated. In the boundary-layer model of Zilitinkevich *et al.* [55], the following relationships between the momentum flux and velocity components in the CBL have been employed:

$$\bar{V} = u_* \frac{a_u + \ln(|L|/z_{0u})}{k}, \quad \bar{u} = \bar{V} \cos \alpha_h, \quad \bar{v} = \bar{V} \sin \alpha_h,$$

$$\sin(\alpha_s - \alpha_h) = \frac{a_\alpha}{k} \left( \frac{h}{|L|} \right)^{-1/3} \frac{u_*}{\bar{V}} \text{sign}f, \quad \tau_{xs} = u_*^2 \cos \alpha_s, \quad \tau_{ys} = u_*^2 \sin \alpha_s,$$

where  $\alpha_h$  is the angle between the  $x$  axis and the velocity vector  $\bar{V}$  with components  $\bar{u}$  and  $\bar{v}$ ,  $\alpha_s$  is the angle between the  $x$  axis and the surface shear stress,  $L = -u_*^2 / (\beta Q_s)$  is the Monin-Obukhov length scale,  $k=0.4$  is the von Karman constant, and  $a_u$  and  $a_\alpha$  are dimensionless parameters for which Zilitinkevich [53] obtained estimates 1 and 3, respectively.

The above expressions constitute a closed set of equations for determination of the components of the near-surface momentum flux, provided  $Q_s$ ,  $\bar{u}$ ,  $\bar{v}$ , and  $z_{0u}$  are known.

The near-surface values of the geostrophic wind components in the atmospheric boundary layer,  $u_{g0}$  and  $v_{g0}$ , can be expressed through the horizontal gradients of the near-surface pressure field  $p_s$  by the well known formulas:

$$u_{g0} = -\frac{1}{f\rho_s} \frac{\partial p_s}{\partial y}, \quad v_{g0} = \frac{1}{f\rho_s} \frac{\partial p_s}{\partial x},$$

where  $\rho_s$  is the near-surface density. Both  $p_s$  and  $\rho_s$  can be evaluated from the weather forecast data, or from the output of some larger-scale atmospheric model.

The vertical variations of the geostrophic wind are usually related to the effects of the so-called thermal wind, which is one of the manifestations of the baroclinicity in the atmosphere. In the CBL, the thermal wind appears as a result of the thermal horizontal nonuniformity of the layer. Under these conditions, the vertical gradients of the geostrophic wind components can be represented as first approximations by

$$\Gamma_u = -\frac{\beta}{f} \frac{\partial \bar{\theta}}{\partial y}, \quad \Gamma_v = \frac{\beta}{f} \frac{\partial \bar{\theta}}{\partial x},$$

following the traditional thermal wind relationship given, *e.g.* in Holton [24], and using the CBL potential temperature averages.

The theory presented in the previous sections of the paper deals with different cases of dry CBL. To account for the effects of air humidity in the unsaturated atmosphere, one should complement the model with the equation of moisture transfer. It is shown in Zilitinkevich *et al.* [55] that the integral humidity budget, and profile of the turbulent flux of moisture in the zero-order CBL model can be expressed in a way analogous to the heat budget and to the heat flux. In the equation terms representing the buoyancy effects, the potential temperature  $\theta$  should be replaced by the virtual potential temperature,  $\theta_v = \theta(1 + 0.61q)$ , where  $q$  is the specific air humidity, and the buoyancy flux has to be written as  $\beta Q + 0.61gE$ , where  $E$  is the kinematic turbulent flux of moisture.

### 3. General Structure Model of the Shear Free CBL

In many instances, the buoyant production of TKE in the atmospheric CBL ultimately dominates the TKE production due to wind shears, so the CBL can be taken as shear-free.

Figure 3 shows the vertical profiles of buoyancy  $b$  and vertical turbulent buoyancy flux  $B$  in the shear-free CBL heated from below. The buoyancy is defined here as  $b = g(\rho_0 - \rho)/\rho_0 \approx g(\theta - \theta_0)/\theta_0$  where  $\rho_0$  is a reference density value. As a result of heating, a well-mixed layer forms in the lower part of the fluid. In the near vicinity of the heated surface, the buoyancy drops sharply from a surface value  $b_s$  to the mixed-layer value  $b_m$ . The homogeneous mixed layer is separated from the nonturbulent layer aloft (which is linearly stratified with the vertical buoyancy gradient  $db/dz = N^2$ ) by the interfacial (entrainment) layer, where the buoyancy increases with height.

The vertical turbulent buoyancy flux  $B$  decreases linearly with height in the main portion of the CBL. Its zero-crossing height roughly defines the mixed-layer depth  $h_0$ . (Note that the mixed-layer depth from the general point of view is different to the CBL depth; only in the zero-order CBL model do these depths coincide.) Being negative over the interfacial layer,  $B$  reaches a minimum within this layer and vanishes towards its upper boundary  $z = h_0 + \Delta h$ . Thus, four regions can be distinguished in the shear-free CBL: the surface layer (whose depth is typically small compared to  $h_0$ ), the mixed layer, the interfacial (entrainment) layer, and the nonturbulent layer.

As can be inferred from the comparison of Fig. 3 and Fig. 1, the buoyancy jump in the zero-order CBL model does not correspond to the actual buoyancy difference across the entrainment layer. It is also possible to show (Fedorovich and Mironov [21]) that the zero-order model value of buoyancy (temperature) flux at the CBL upper edge is not equal to the most negative flux of entrainment presented in Fig. 3.

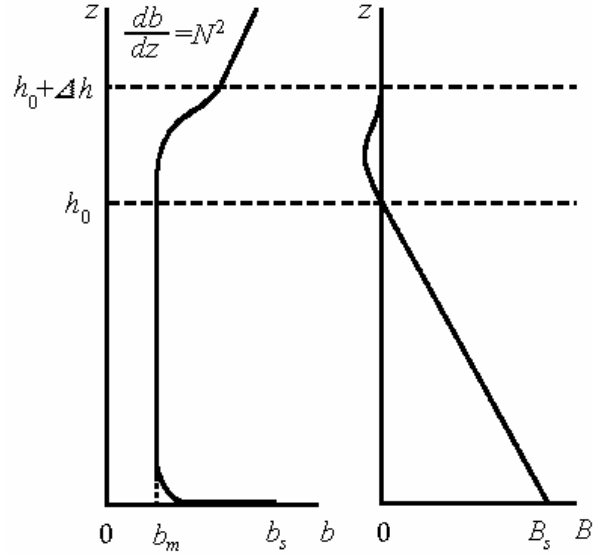


Figure 3. Vertical profiles of buoyancy  $b$  and turbulent buoyancy flux  $B$  in the shear-free CBL.

Based upon the experimental evidence that the buoyancy increment in the upper portion of the CBL occurs over a layer of significant thickness, Betts [5] proposed the so-called first-order jump CBL model. The model assumes that the mixed layer extends up to the height of the most negative buoyancy flux of entrainment, and that  $b$  and  $B$  increase linearly with height throughout the interfacial layer, undergoing the first-order discontinuities at its upper and lower boundaries. However, one can note from Fig. 3 that the profiles of  $b$  and  $B$  in the interfacial layer are hardly the linear ones in reality, and that the minimum buoyancy flux of entrainment occurs within the interfacial layer, not at its bottom. Consequently, the interfacial-layer thickness in the first-order jump model is significantly smaller than the actual one.

The next step towards more realistic parameterization of the entrainment zone was made by Deardorff [13] who allowed all negative buoyancy flux of entrainment to take place within the entrainment layer. The entrainment-layer buoyancy profile in the Deardorff model is represented as

$$b = b_m + F\Delta b, \quad (20)$$

where  $F$  is a dimensionless function of height. The normalized integral of this function over the entrainment layer (the integral shape factor),

$$C_b = \Delta h^{-1} \int_{h_0}^{h_0 + \Delta h} F dz, \quad (21)$$

is assumed to be dependent on relative stratification  $G = N^2 (\Delta h / \Delta b)$ , *i.e.* on the square of the ratio of  $N$  and the mean buoyancy frequency in the IL,  $(\Delta b / \Delta h)^{1/2}$ . The empirical approximation of  $C_b(G)$  was suggested in Deardorff [13], however, the form of the function  $F$  was not determined.

The Deardorff general-structure CBL model performed well in the cases of steady-state entrainment with large-scale subsidence ( $d h_0 / dt = d \Delta h / dt = d \Delta b / dt = 0$ ) and pseudoencroachment ( $d \Delta h / dt = d \Delta b / dt = 0$  and  $G=1$ ), when no closure assumption on  $d h_0 / dt$  or  $d \Delta h / dt$  was required. For unsteady entrainment, a quite arbitrary closure assumption was made concerning  $d \Delta h / dt$  which looks more like a fitting relation than a theoretically substantiated equation. Furthermore, this relation provides an ambiguous expression for  $d \Delta h / dt$  when  $\Delta b$  and  $\Delta h$  become small.

Following the model line of Deardorff [13], Fedorovich and Mironov [21] derived rate equations for  $h_0$  and  $\Delta h$  departing from the TKE balance equation and using the Deardorff [10] hypothesis of similarity for convective boundary layers revised to account for the entrainment-layer structure. They also attempted to find a reasonable approximation for the buoyancy profile within the IL.

The general-structure CBL model of Fedorovich and Mironov [21] and some results from their study are presented in the following subsections of the paper.

### 3.1. BUOYANCY BUDGET

We simplify the discussion by considering a horizontally homogeneous boundary layer without a large-scale subsidence. Let us assume that with the development of convection the vertical buoyancy profile in the CBL keeps the following form:

$$b = \begin{cases} b_m & \text{at } 0 \leq z \leq h_0, \\ b_m + \Delta b F(\zeta, G) & \text{at } h_0 \leq z \leq h_0 + \Delta h, \\ b_m + \Delta b + N^2(z - h_0 - \Delta h) & \text{at } h_0 + \Delta h \leq z. \end{cases} \quad (22)$$

The quiescence of the turbulence-free layer above the CBL is adopted in the model. This implies that in the free atmosphere some initial linear buoyancy profile  $b_0(z)$  is conserved, so that  $b(z, t) = b_0(z)$  at  $z \geq h_0 + \Delta h$ .

In the representation (22),  $F$  is a function of the dimensionless coordinate  $\zeta = (z - h_0) / \Delta h$  and stratification parameter  $G$ . It satisfies the following boundary conditions:

$$F|_{\zeta=0} = \frac{\partial F}{\partial \zeta}|_{\zeta=0} = 0, \quad F|_{\zeta=1} = 1, \quad \frac{\partial F}{\partial \zeta}|_{\zeta=1} = G. \quad (23)$$

The parameterization (22) omits the difference between  $b_m$  and the buoyancy in the thin near-surface layer, (see Fig. 3). Its small contribution to the total buoyancy budget in the shear-free CBL can be neglected.

The evolution of the buoyancy profile (3) should satisfy the buoyancy transfer equation

$$\frac{\partial b}{\partial t} = -\frac{\partial B}{\partial z}. \quad (24)$$

Integrating Eq. (24) over  $z$  from 0 to  $h_0$  with due regard to the representation (22) and taking into account the definition of the mixed-layer depth as the buoyancy flux crossover height, *i.e.*  $B=0$  at  $z=h_0$ , we obtain the equation of the mixed-layer buoyancy budget, (see Fedorovich and Mironov [21] for details of derivation),

$$\frac{d}{dt} [N^2(h_0 + \Delta h) - \Delta b] = \frac{B_s}{h_0}. \quad (25)$$

Integration of Eq. (24) over  $z$  from 0 to  $h_0 + \Delta h$  gives the equation of total buoyancy budget in the CBL:

$$\frac{d}{dt} \left\{ \frac{1}{2} N^2 (h_0 + \Delta h)^2 - \Delta b [h_0 + (1 - C_b) \Delta h] \right\} = B_s, \quad (26)$$

where  $C_b(G) = \int_0^1 F(\zeta, G) d\zeta$  is the integral shape factor, see Eq. (21).

Equations (25) and (26) are the two ordinary differential equations for three unknowns:  $h_0$ ,  $\Delta h$  and  $\Delta b$ . An additional expression relating these variables is needed to close the problem.

### 3.2. ENTRAINMENT RATE EQUATION

The closure equation can be derived departing from the TKE balance in the shear-free CBL:

$$\partial e / \partial t = B - \partial \Phi / \partial z - \varepsilon. \quad (27)$$

We adopt the hypothesis of similarity of the convective regime considered. This hypothesis states that the basic turbulence parameters, being normalized by the length

scale  $h_0 + \Delta h$  and the velocity scale  $w_* = [B_s(h_0 + \Delta h)]^{1/3}$ , cease to depend on time in their explicit form and depend on it only through these scales, *i.e.* they become universal functions of the dimensionless height  $z/(h_0 + \Delta h)$ . Hence, the vertical profiles of turbulent energy and its dissipation rate can be presented in the form:

$$e = w_*^2 F_e \left( \frac{z}{h_0 + \Delta h} \right), \quad \varepsilon = \frac{w_*^3}{h_0 + \Delta h} F_\varepsilon \left( \frac{z}{h_0 + \Delta h} \right), \quad (28)$$

where  $F_e$  and  $F_\varepsilon$  are dimensionless functions satisfying the boundary conditions  $F_e(1) = F_\varepsilon(1) = 0$ .

The employed closure hypothesis is very similar to the one proposed by Deardorff [10] which has been widely used in the CBL zero-order jump models. However, instead of an arbitrary height within the limits of the interfacial layer (usually corresponding to the elevation of buoyancy flux minimum), we use  $h_0 + \Delta h$ , *i.e.* the whole CBL depth, as an appropriate length scale. Fedorovich and Mironov [21] have shown that employment of  $h_0 + \Delta h$  as the length scale allows one to decrease the range of empirical estimates of the universal functions for  $\varepsilon$  and  $e$  in the upper portion of the CBL.

The termwise integration of Eq. (27) over  $z$  from 0 to  $h_0 + \Delta h$  leads to the following equation relating  $h_0$ ,  $\Delta h$  and  $\Delta b$  (Fedorovich and Mironov [21]):

$$\begin{aligned} \frac{10}{3} C_e \left( 1 + \frac{\Delta h}{h_0} \right)^{2/3} (E_h + E_\Delta) &= (1 - 2C_\varepsilon) - 2C_\varepsilon \frac{\Delta h}{h_0} - \left( 1 - 2C_{bb} + 2G \frac{dC_{bb}}{dG} \right) \left( \frac{\Delta h}{h_0} \right)^2 + \\ &+ 2 \left( C_b - GC_{bb} + G^2 \frac{dC_{bb}}{dG} \right) \frac{\Delta h}{h_0} \text{Ri}_b E_h + \\ &+ 2 \left[ C_b - 2C_{bb} - GC_{bb} - G(1 - G) \frac{dC_{bb}}{dG} \right] \frac{\Delta h}{h_0} \text{Ri}_b E_\Delta - \\ &- \frac{4}{3} C_e \left( 1 + \frac{\Delta h}{h_0} \right)^{5/3} \text{De} - 2 \frac{\Phi(h_0 + \Delta h)}{B_s h_0}, \end{aligned} \quad (29)$$

where  $E_h = (B_s h_0)^{-1/3} dh_0 / dt$  is the dimensionless rate of  $h_0$  change;  $E_\Delta = (B_s h_0)^{-1/3} d\Delta h / dt$  is the dimensionless rate of  $\Delta h$  change;  $\text{Ri}_b = B_s^{-2/3} h_0^{1/3} \Delta b$  is the Richardson number based on  $h_0$  and buoyancy increment  $\Delta b$  across the IL;  $\text{De} = B_s^{-4/3} h_0^{2/3} dB_s / dt$  is the nonstationarity parameter introduced in Deardorff *et al.* [16];  $C_e = \int_0^1 F_e(x) dx$  and  $C_\varepsilon = \int_0^1 F_\varepsilon(x) dx$  are dimensionless constants;

$C_{bb} = \int_0^1 d\zeta \int_0^\zeta F(\zeta', G) \zeta'$  is a dimensionless function of  $G$ ;  $\Phi(h_0 + \Delta h)$  is the energy flux at the boundary layer top.

The latter can be evaluated evoking the relationships proposed either by Kantha [25] or by Zilitinkevich [54], see section 2.3. In terms of the general-structure CBL model, the first of these relationships yields

$$2 \frac{\Phi(h_0 + \Delta h)}{B_s h_0} = C_N \text{Ri}_N^{3/2} \left( \frac{\Delta h}{h_0} \right)^2, \quad (30)$$

and the second results in

$$2 \frac{\Phi(h_0 + \Delta h)}{B_s h_0} = C_N' \text{Ri}_N^{3/2} \left( \frac{\Delta h}{h_0} \right)^3, \quad (31)$$

where  $\text{Ri}_N = B_s^{-2/3} h_0^{4/3} N^2$  is the Richardson number based on  $h_0$  and  $N$ , and  $C_N$  and  $C_N'$  are dimensionless constants.

Equations (25), (26), (29), (30) or (31) constitute a closed set. The dimensionless constants  $C_\varepsilon$ ,  $C_e$ ,  $C_N$  or  $C_N'$ , and the shape factors  $C_b(G)$  and  $C_{bb}(G)$  have been determined by Fedorovich and Mironov [21] from data of atmospheric, oceanic, laboratory, and LES studies of the shear-free CBL.

An approximation of the function  $F(\zeta, G)$ , fitting experimental and model data reasonably well, was obtained in [21] from geometrical arguments. To match the continuity conditions (23), the required function was represented in the form of a fourth-order polynomial. Coefficients of this polynomial were set to be functions of  $C_b$  in order to satisfy the additional integral condition (21). This provided the following approximation for the dimensionless buoyancy profile in the entrainment zone:

$$F(\zeta, G) = \left( \frac{3}{2} G - 12 + 30C_b \right) \zeta^2 + (28 - 4G - 60C_b) \zeta^3 + \left( \frac{5}{2} G - 15 + 30C_b \right) \zeta^4, \quad (32)$$

where the dependence of the integral shape factor  $C_b$  on the relative stratification  $G$  was given by

$$C_b = 0.55 \exp(-0.27G). \quad (33)$$

The last expression, which had been originally proposed by Deardorff [13], was verified by Fedorovich and Mironov [21] against data collected from a variety of CBL experimental and model studies.

## 3.3. MODELING LABORATORY CBL

The pure case of the shear-free CBL was simulated in the series of water-tank experiments by Deardorff *et al.* ([15], [16], Willis and Deardorff [50], Deardorff and Willis [14]). The most comprehensive data set was presented in Deardorff *et al.* [16] hereafter referred to as DWS. It was used by Fedorovich and Mironov [21] to test their general-structure CBL model.

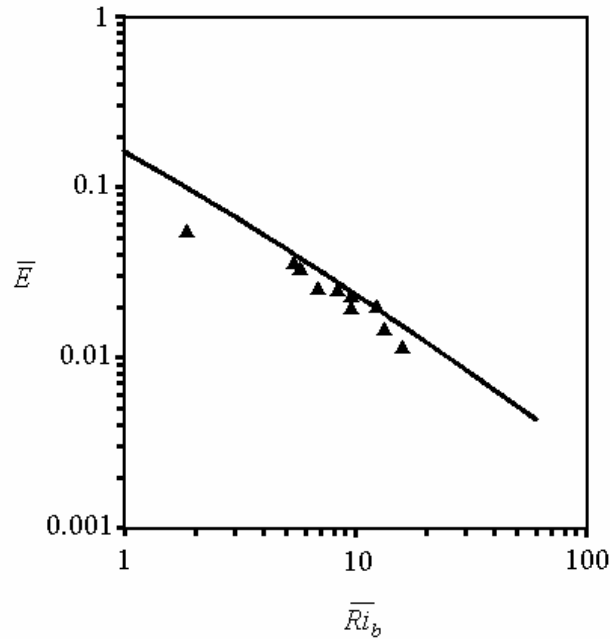


Figure 4. Dimensionless entrainment rate versus the Richardson number for a two-layer fluid system. The model curve from [21] is shown by the solid line; the points are the DWS results.

Following the DWS notation originating from the zero-order jump approach, we will express parameters of entrainment in terms of  $\bar{h}$ , which is the elevation of buoyancy-flux minimum within the entrainment zone:

$$\bar{E} = (B_s \bar{h})^{-1/3} d\bar{h} / dt, \quad \bar{Ri}_b = B_s^{-2/3} \bar{h}^{1/3} \Delta b, \quad \bar{Ri}_N = \frac{1}{2} B_s^{-2/3} \bar{h}^{4/3} N^2. \quad (34)$$

The general-structure model allows the determination of  $\bar{h}$  directly from the shape of the buoyancy flux profile.

Predictions of entrainment rate by the general-structure CBL model agree well with the data from the DWS two-layer fluid experiments, see Fig. 4. The two-layer fluid case corresponds to neutral stratification in the free atmosphere above the CBL ( $\overline{Ri}_N = 0$ ). Here we use the traditional terminology, speaking about a "two-layer fluid", although in reality it is a three-layer one: mixed layer - interfacial layer - nonturbulent neutral layer. Within the zero-order approach, this is really a two-layer fluid because the interfacial layer is reduced to the zero-thickness surface. The calculated dependence of  $\overline{E}$  on  $\overline{Ri}_b$  practically coincides with the basic relation of the zero-order model for convection in the two-layer fluid:  $\overline{E} \cdot \overline{Ri}_b = const.$

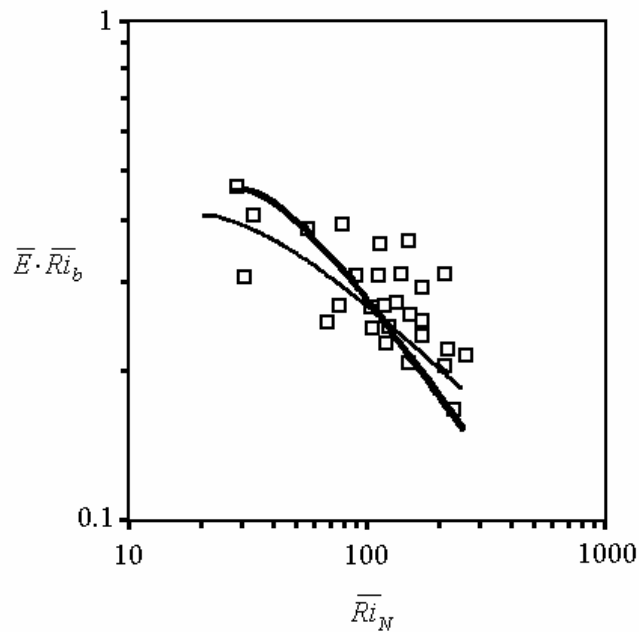
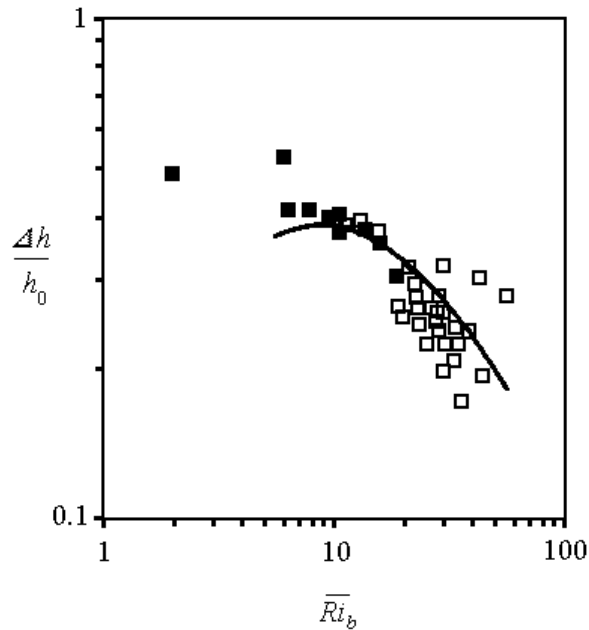


Figure 5. Entrainment in the linearly stratified fluid. The heavy solid curve is calculated using Eq. (30), the solid line shows the results of calculation with Eq. (31); the points are the DWS data.

If the nonturbulent layer above the CBL is stably stratified, the entrainment law relates  $\overline{E}$  to two Richardson numbers,  $\overline{Ri}_b$  and  $\overline{Ri}_N$ . In Fig. 5, the product  $\overline{E} \cdot \overline{Ri}_b$  is plotted against  $\overline{Ri}_N$ . Model curves presented in the plot were obtained using two parameterizations, (30) and (31), for wave-related energy flux at the boundary-layer top. The dimensionless constants  $C_N = 0.001$  and  $C_N' = 0.012$  were estimated in [21] as

the best fit to empirical data from the DWS experiments with the linearly stratified fluid. The overall difference between the two parameterizations in Fig. 5 is rather small considering the data scatter. Still, the DWS data gives more proof to Eq. (31), than to Eq. (30).



*Figure 6.* Normalized entrainment layer depth versus the Richardson number in the linearly stratified fluid. The curve is calculated by the general-structure CBL model with the energy flux parameterized after (31). The open squares represent the DWS data referring to a linearly stratified fluid. The DWS data from experiments intended to treat a two-layer fluid system are shown by filled squares.

The DWS experiments with a two-layer fluid were actually performed in the presence of weak stable density stratification in the quiescent layer. This can be inferred from parameters of the experimental setup tabulated in [16]. Calculations with the general-structure model [21] showed that the effect of this stratification could be, nevertheless, strong enough to modify the regime of entrainment compared to the pure case of convection in the two-layer fluid. The  $\Delta h/h_0$  values from the DWS experiments are plotted against  $\overline{Ri}_b$  in Fig. 6 with due regard to non-zero values of  $N^2$ . They conform fairly well with the theoretical curve for a linearly stratified fluid at small  $\overline{Ri}_b$ .

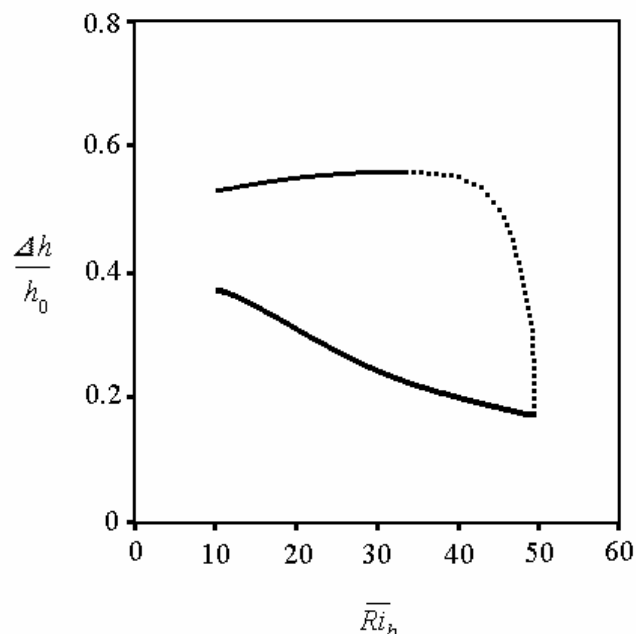


Figure 7. Convective boundary layer development in a composite stratified flow. The heavy solid curve corresponds to the entrainment in a linearly stratified layer. The dashed curve represents the transition stage of the boundary layer development when the entrainment adjusts to a regime characteristic of a two-layer system. The solid line displays the quasi-equilibrium entrainment in a two-layer fluid.

With the aid of the general-structure CBL model, Fedorovich and Mironov [21] found that nonstationarity of the entrainment zone can essentially modify relationships between the entrainment parameters in the shear-free CBL. Figure 7 shows the numerical results for the CBL growing through a stratified flow composed of linearly stratified lower layer and neutrally stratified upper layer. The entrainment occurs first in a linearly stratified fluid, where  $\Delta h/h_0$  decreases monotonously with  $\overline{Ri}_b$  (heavy solid curve). After the entrainment-layer top has reached the base of the neutral layer, the entrainment zone passes through a transition stage (dashed curve) towards a quasi-equilibrium state characteristic of a two-layer fluid. At the transition stage of entrainment,  $\Delta h/h_0$  reveals inverse dependence on  $\overline{Ri}_b$  as compared with the quasi-equilibrium entrainment regime in a nearly neutral fluid (solid curve).

The model curve in Fig. 7 forms nearly a closed loop. A similar behavior of the interdependencies of the entrainment parameters was observed in the day-time atmospheric boundary layer by Nelson *et al.* [36], who called this phenomenon the hysteresis of the entrainment zone.

#### 4. Summary

We have presented two typical CBL bulk models: the zero-order jump model and the general-structure CBL model.

The zero-order CBL model proves to be a useful tool for applied studies of the atmospheric CBL. Wind engineering and pollutant-dispersion modeling can be mentioned as prospective areas for the application of the zero-order jump approach.

Despite the simplicity of zero-order jump model approach, it provides the opportunity of accounting for a variety of physical mechanisms determining the temporal and spatial structure of the atmospheric CBL. The model allows a generalization for the CBL over irregular terrain. Further progress in zero-order CBL modeling essentially depends on success in developing scalings and parameterizations for different turbulence regimes in the atmospheric CBL.

The general-structure CBL model is based on the realistic representation of the buoyancy profile throughout the entrainment zone of the shear-free CBL. The explicit self-similar representation of this profile was proposed. The integral shape factor of the profile was shown to be a universal function of the dimensionless stratification parameter relating buoyancy gradients above and across the entrainment zone.

The general-structure model approach allows the simulation of entrainment-zone dynamics and description of transition entrainment regimes in multilayer flows. The model successfully reproduces basic shear-free CBL cases simulated in the laboratory experiments of Deardorff *et al.*, and provides theoretical explanations for particular cases of the atmospheric shear-free convection affected by nonstationarity of the entrainment zone.

#### References

1. Ball, F. K. (1960) Control of inversion height by surface heating, *Quart. J. Roy. Meteorol. Soc.*, **86**, 483-494.
2. Batchvarova, E. and Gryning, S.-E. (1991) Applied model for the growth of the daytime mixed layer, *Bound.-Layer Meteor.*, **56**, 261-274.
3. Batchvarova, E. and Gryning, S.-E. (1994) An applied model for the height of the daytime mixed layer and the entrainment zone, *Bound.-Layer Meteor.*, **71**, 311-323.
4. Betts, A.K. (1973) Non-precipitating cumulus convection and its parameterization. *Quart. J. Roy. Meteorol. Soc.*, **99**, 178-196.
5. Betts, A. K. (1974) Reply to comment on the paper "Non-precipitating cumulus convection and its parameterization", *Quart. J. Roy. Meteorol. Soc.*, **100**, 469-471.
6. Brutsaert, W. (1987) Nearly steady convection and the boundary layer budgets of water vapor and sensible heat, *Bound.-Layer Meteor.*, **39**, 283-300.
7. Carson, D. J. (1973) The development of dry inversion-capped convectively unstable boundary layer, *Quart. J. Roy. Meteorol. Soc.*, **99**, 450-467.
8. Carson, D. J., and Smith, F. B. (1974) Thermodynamic model for the development of a convectively unstable boundary layer, in H. E. Landsberg and J. Van Mieghem (eds.), *Advances in Geophysics*, **18A**, Academic Press, pp. 111-124.
9. Deardorff, J. W. (1970) Preliminary results from numerical integration of the unstable boundary layer, *J. Atmos. Sci.*, **27**, 1209-1211.

10. Deardorff, J. W. (1970) Convective velocity and temperature scales for the unstable planetary boundary layer and for Raleigh convection, *J. Atmos. Sci.*, **27**, 1211-1213.
11. Deardorff, J. W. (1972) Numerical investigation of neutral and unstable planetary boundary layers, *J. Atmos. Sci.*, **29**, 91-115.
12. Deardorff, J. W. (1974) Tree dimensional numerical study of turbulence in an entraining mixed layer, *Bound.-Layer Meteor.*, **7**, 199-226.
13. Deardorff, J. W. (1979) Prediction of convective mixed-layer entrainment for realistic capping inversion structure, *J. Atmos. Sci.*, **36**, 424-436.
14. Deardorff, J. W., and Willis, G. E. (1985) Further results from a laboratory model of the convective planetary boundary layer, *Bound.-Layer Meteor.*, **32**, 205-236.
15. Deardorff, J. W., Willis, G. E., and Lilly, D. K. (1969) Laboratory investigation of non-steady penetrative convection, *J. Fluid Mech.*, **35**, 7-31.
16. Deardorff, J. W., Willis, G. E., and Stockton, B. H. (1980) Laboratory studies of the entrainment zone of a convectively mixed layer, *J. Fluid Mech.*, **100**, 41-64.
17. Driedonks, A. G. M. (1982) Models and observations of the growth of the atmospheric boundary layer, *Bound.-Layer Meteor.*, **23**, 283-306.
18. Driedonks, A. G. M. and Tennekes, H. (1984) Entrainment effects in the well-mixed atmospheric boundary layer, *Bound.-Layer Meteor.*, **30**, 75-103.
19. Fedorovich, E. (1995) Modeling the atmospheric convective boundary layer within a zero-order jump approach: an extended theoretical framework, *J. Appl. Meteor.*, **34**, 1916-1928.
20. Fedorovich, E. and Kaiser, R. (1998) Wind tunnel model study of turbulence regime in the atmospheric convective boundary layer. See this volume.
21. Fedorovich, E. E. and Mironov, D. V. (1995) A model for a shear-free convective boundary layer with parameterized capping inversion structure, *J. Atmos. Sci.*, **52**, 83-95.
22. Garrat, J. R., Wyngaard, J. C., and Francey, R. J. (1982) Winds in the atmospheric boundary layer – prediction and observation, *J. Atmos. Sci.*, **39**, 1307-1316.
23. Gryning, S.-E. and Batchvarova, E. (1994) Parameterization of the depth of the entrainment zone above the daytime mixed layer, *Quart. J. Roy. Meteorol. Soc.*, **120**, 47-58.
24. Holton, J. R. (1972) *An Introduction to Dynamic Meteorology*, Academic Press.
25. Kantha, L. H. (1977) Note on the role of internal waves in thermocline erosion, in E. B. Kraus (ed.), *Modelling and predictions of the upper layer of the ocean*, Pergamon Press, pp. 173-177.
26. Kraus, E. B. and Leslie, L. D. (1982) The interactive evolution of the oceanic and atmospheric boundary layers in the source regions of the trades, *J. Atmos. Sci.*, **39**, 2760-2772.
27. Lenschow, D. (1998) Observations of clear and cloud-capped convective boundary layers, and techniques for probing them. See this volume.
28. Lenschow, D. H., Wyngaard, J. C., and Pennel, W. T. (1980) Mean-field and second-momentum budgets in a baroclinic, convective boundary layer, *J. Atmos. Sci.*, **37**, 1313-1326.
29. Lilly, D. K. (1968) Models of cloud-topped mixed layers under a strong inversion, *Quart. J. Roy. Meteorol. Soc.*, **94**, 292-309.
30. Mason, P. J. (1989) Large-eddy simulation of the convective atmospheric boundary layer, *J. Atmos. Sci.*, **46**, 1492-1516.
31. Moeng, C.-H. (1984) A large-eddy simulation for the study of planetary boundary layer turbulence, *J. Atmos. Sci.*, **41**, 2052-2062.
32. Moeng, C.-H. (1986) Large-eddy simulation of a stratus-topped boundary layer. Part I: Structure and budgets, *J. Atmos. Sci.*, **43**, 2886-2900.
33. Moeng, C.-H. (1987) Large-eddy simulation of a stratus-topped boundary layer. Part II: Implications for mixed-layer modeling, *J. Atmos. Sci.*, **44**, 1606-1614.
34. Moeng, C.-H. and Sullivan, P.P. (1994) A comparison of shear- and buoyancy-driven planetary boundary layer flows, *J. Atmos. Sci.*, **51**, 999-1022.
35. Moeng, C.-H. and Wyngaard, J. C. (1988) Spectral analysis of large-eddy simulations of the convective boundary layer, *J. Atmos. Sci.*, **45**, 3574-3587.
36. Nelson, E., Stull, R., and Eloranta, E. (1989) A prognostic relationship for entrainment zone thickness, *J. Appl. Meteorol.*, **28**, 885-903.
37. Nieuwstadt, F. T. M. and Brost, R. A. (1986) Decay of convective turbulence, *J. Atmos. Sci.*, **43**, 532-546.

38. Plate, E. J. (1971) *Aerodynamic Characteristics of Atmospheric Boundary Layers*, US Atomic Energy Commission, Oak Ridge, Tennessee.
39. Plate, E. J. (1998) Convective boundary layer: a historical introduction. See this volume.
40. Qi, Y., Zhou, J., and Fu, B. (1994) Airflow over a mountain and the convective boundary layer, *Bound.-Layer Meteor.*, **68**, 301-318.
41. Schmidt, H. and Schumann, U. (1989) Coherent structure of the convective boundary layer derived from large-eddy simulations, *J. Fluid. Mech.*, **200**, 511-562.
42. Stull, R. B. (1973) Inversion rise model based on penetrative convection, *J. Atmos. Sci.*, **30**, 1092-1099.
43. Stull, R. B. (1976) The energetics of entrainment across a density interface, *J. Atmos. Sci.*, **33**, 1260-1267.
44. Stull, R. B. (1976) Mixed-layer depth model based on turbulent energetics, *J. Atmos. Sci.*, **33**, 1268-1278.
45. Stull, R. B. (1976) Internal gravity waves generated by penetrative convection, *J. Atmos. Sci.*, **33**, 1279-1286.
46. Stull, R. B. (1988) *An Introduction to Boundary Layer Meteorology*, Kluwer, Dordrecht.
47. Tennekes, H. (1973) A model for the dynamics of the inversion above a convective boundary layer, *J. Atmos. Sci.*, **42**, 558-567.
48. Tennekes, H. and Driedonks, A. J. M. (1981) Basic entrainment equations for the atmospheric boundary layer, *Bound.-Layer Meteor.*, **20**, 515-531.
49. Thorpe, S. A. (1973) Turbulence in stably stratified fluids: a review of laboratory experiments, *Bound.-Layer Meteor.*, **5**, 95-119.
50. Willis, G.E. and Deardorff, J. W. (1974) A laboratory model of the unstable planetary boundary layer, *J. Atmos. Sci.*, **31**, 1297-1307.
51. Zeman, O. and Tennekes, H. (1977) Parameterization of the turbulent energy budget at the top of the daytime atmospheric boundary layer, *J. Atmos. Sci.*, **34**, 111-123.
52. Zilitinkevich, S. S. (1975) Comments on "A model for the dynamics of the inversion above a convective boundary layer", *J. Atmos. Sci.*, **32**, 991-992.
53. Zilitinkevich, S. S. (1975) Resistance laws and prediction equations for the depth of the planetary boundary layer, *J. Atmos. Sci.*, **32**, 741-752.
54. Zilitinkevich, S. S. (1991) *Turbulent Penetrative Convection*, Avebury Technical, Aldershot.
55. Zilitinkevich, S. S., Fedorovich, E. E., and Shabalova, M. V. (1992) Numerical model of a non-steady atmospheric planetary boundary layer, based on similarity theory, *Bound.-Layer Meteor.*, **59**, 387-411.